

## Protonium annihilation into $\pi^0\pi^0$ at rest in a liquid hydrogen target

M. Bargiotti,<sup>1</sup> A. Bertin,<sup>1</sup> M. Bruschi,<sup>1</sup> M. Capponi,<sup>1</sup> S. De Castro,<sup>1</sup> R. Donà,<sup>1</sup> L. Fabbri,<sup>1</sup> P. Faccioli,<sup>1</sup> D. Galli,<sup>1</sup> B. Giacobbe,<sup>1</sup> U. Marconi,<sup>1</sup> I. Massa,<sup>1</sup> M. Piccinini,<sup>1</sup> N. Semprini Cesari,<sup>1</sup> R. Spighi,<sup>1</sup> V. Vagnoni,<sup>1</sup> S. Vecchi,<sup>1</sup> M. Villa,<sup>1</sup> A. Vitale,<sup>1</sup> A. Zoccoli,<sup>1</sup> M. Poli,<sup>2</sup> G. Bonomi,<sup>3</sup> M. P. Busa,<sup>3</sup> M. Corradini,<sup>3</sup> E. Lodi Rizzini,<sup>3</sup> L. Venturini,<sup>3</sup> A. Zenoni,<sup>3</sup> C. Cicalò,<sup>4</sup> A. De Falco,<sup>4</sup> A. Masoni,<sup>4</sup> G. Puddu,<sup>4</sup> S. Serci,<sup>4</sup> G. Usai,<sup>4</sup> O. E. Gorchakov,<sup>5</sup> S. N. Prakhov,<sup>5</sup> A. M. Rozhdestvensky,<sup>5</sup> V. I. Tretyak,<sup>5</sup> P. Gianotti,<sup>6</sup> C. Guaraldo,<sup>6</sup> A. Lanaro,<sup>6</sup> V. Lucherini,<sup>6</sup> C. Petrascu,<sup>6</sup> R. A. Ricci,<sup>7</sup> V. Filippini,<sup>8</sup> A. Fontana,<sup>8</sup> P. Montagna,<sup>8</sup> A. Rotondi,<sup>8</sup> P. Salvini,<sup>8</sup> F. Balestra,<sup>9</sup> P. Cerello,<sup>9</sup> O. Denisov,<sup>9</sup> L. Ferrero,<sup>9</sup> R. Garfagnini,<sup>9</sup> A. Grasso,<sup>9</sup> A. Maggiora,<sup>9</sup> A. Panzarasa,<sup>9</sup> D. Panzieri,<sup>9</sup> F. Tosello,<sup>9</sup> M. Astrua,<sup>10</sup> E. Botta,<sup>10</sup> T. Bressani,<sup>10</sup> D. Calvo,<sup>10</sup> A. Feliciello,<sup>10</sup> A. Filippi,<sup>10</sup> N. Mirfakhrai,<sup>10,\*</sup> S. Marcello,<sup>10</sup> M. Agnello,<sup>11</sup> and F. Iazzi<sup>11</sup>

(OBELIX Collaboration)

<sup>1</sup>Dipartimento di Fisica dell'Università di Bologna and INFN Sezione di Bologna, Bologna, Italy

<sup>2</sup>Dipartimento di Energetica dell'Università di Firenze, Firenze Italy  
and INFN Sezione di Bologna, Bologna, Italy

<sup>3</sup>Dipartimento di Chimica e Fisica per i Materiali, Università di Brescia, Brescia, Italy  
and INFN Sezione di Pavia, Pavia, Italy

<sup>4</sup>Dipartimento di Scienze Fisiche, Università di Cagliari and INFN Sezione di Cagliari, Cagliari, Italy

<sup>5</sup>Joint Institute for Nuclear Research, Dubna, Russia

<sup>6</sup>Lab. Naz. di Frascati dell'INFN, Frascati, Italy

<sup>7</sup>Lab. Naz. di Legnaro dell'INFN, Legnaro, Italy

<sup>8</sup>Dipartimento di Fisica Nucleare e Teorica dell'Università di Pavia and INFN Sezione di Pavia, Pavia, Italy

<sup>9</sup>Dipartimento di Fisica Generale dell'Università di Torino and INFN Sezione di Torino, Torino, Italy

<sup>10</sup>Dipartimento di Fisica Sperimentale dell'Università di Torino and INFN Sezione di Torino, Torino, Italy

<sup>11</sup>Dipartimento di Fisica del Politecnico di Torino and INFN Sezione di Torino, Torino, Italy

(Received 8 August 2001; published 11 December 2001)

The annihilation frequency of the reaction  $\bar{p}p \rightarrow \pi^0\pi^0$  at rest in liquid hydrogen has been measured by the Obelix experiment by using different apparatus configurations and trigger conditions. The value obtained is  $f(\pi^0\pi^0, \text{LH}) = (2.8 \pm 0.1_{\text{stat}} \pm 0.4_{\text{syst}}) \times 10^{-4}$ . With the same data samples, the  $\pi^0\eta$  annihilation frequency has been determined to be  $f(\pi^0\eta, \text{LH}) = (0.9 \pm 0.2_{\text{stat}} \pm 0.1_{\text{syst}}) \times 10^{-4}$ . The results are discussed within the frame of the present experimental situation.

DOI: 10.1103/PhysRevD.65.012001

PACS number(s): 13.75.Cs, 36.10.Gv

### I. INTRODUCTION

The measurement of the protonium annihilation frequencies ( $f$ ) into two-body final states is relevant both to the knowledge of the protonium  $J^{PC}$  initial state distribution and to the studies on annihilation dynamics. For this reason, the last generation experiments operating at LEAR carried out an extensive program of measurements in this field. Important information can be obtained both from the direct comparison of  $f$  for specific channels (as  $\pi^+\pi^-$ ,  $\pi^0\pi^0$  and  $K_S K_L$ ) [1] and by studying the whole set of experimental results under some generally accepted hypotheses [2–6]. In this context, the annihilation frequencies of the reactions  $\bar{p}p \rightarrow \pi^0\pi^0$  and  $\bar{p}p \rightarrow \pi^0\eta$  at rest have a particular importance, because they can proceed only from the  $^3P_0$  and  $^3P_2$  protonium initial states and their measurements can provide a direct evaluation of the protonium  $P$ -wave percentage at a given density. We recall here that the experimental branching ratios of the mesons produced in the  $\bar{p}p$  annihilation at rest, as determined by spin-parity analyses, in some cases depend on *a priori* assumptions on this percentage [7].

The present experimental situation concerning the measurements of  $f(\pi^0\pi^0, \rho)$  in liquid hydrogen (LH;  $\rho$  is the target density), summarized in Table I and represented in Fig. 1, is quite contradictory [1,8–14]; in particular, the results from Crystal Barrel (CB) [8], confirmed by a recent reanalysis [9], are more than a factor of 2 larger than the average of the previous ones. At the moment, results in gaseous hydrogen have been obtained only by Obelix [1] in normal temperature and pressure (NTP) conditions (GH or  $\rho_{\text{NTP}}$ ) and by Crystal Barrel [9] at  $12\rho_{\text{NTP}}$ .

In this paper, we describe the new measurements of the  $\pi^0\pi^0$  and  $\pi^0\eta$  annihilation frequencies at rest in LH performed by the Obelix experiment. The previously quoted  $f(\pi^0\pi^0, \rho)$  measurement by Obelix in NTP conditions offers the opportunity of observing this reaction in different target conditions, therefore allowing important cross-checks and helping in the control of the systematic errors.

The  $f(\pi^0\pi^0, \text{LH})$  annihilation frequency has been measured by detecting the  $4\gamma$  final state and by applying several analysis methods, making use of data samples with different trigger conditions and apparatus configurations. The main  $\pi^0\pi^0$  measurement, performed by means of a neutral trigger, has been cross-checked twice: first, by analyzing the minimum bias (MB) data collected in the same experimental conditions and, successively, by using another MB sample col-

\*Present address: Shahid Beheshti University, Teheran, Iran.

TABLE I. Present experimental situation of the  $\bar{p}p \rightarrow \pi^0 \pi^0$  annihilation frequency at rest. LH and GH stand, respectively, for liquid hydrogen and gaseous hydrogen in NTP conditions.

$f(\bar{p}p \rightarrow \pi^0 \pi^0, \rho) (\times 10^{-4})$	Year	Target density	Ref.
$4.8 \pm 1.0$	1971	LH	Devons <i>et al.</i> [10]
$1.4 \pm 0.3$	1979	LH	Bassompierre <i>et al.</i> [11]
$6.0 \pm 4.0$	1983	LH	Backenstoss <i>et al.</i> [12]
$2.06 \pm 0.14$	1987	LH	Adiels <i>et al.</i> [13]
$2.5 \pm 0.3$	1988	LH	Chiba <i>et al.</i> [14]
$6.93 \pm 0.47$	1992	LH	C.B. (AN) [8]
$6.14 \pm 0.40$	2001	LH	C.B. (MB) [9]
$2.8 \pm 0.4$	2001	LH	This work
$12.7 \pm 2.1$	1994	GH	Obelix (AN) [1]
$15.4 \pm 0.9$	2001	$12\rho_{\text{NTP}}$	C.B. (MB) [9]

lected with completely different beam line and target setup one year later.

The  $\pi^0 \pi^0$  annihilation frequency is determined by the following relation:

$$f(\pi^0 \pi^0, \text{LH}) = \frac{N_{\pi^0 \pi^0} - N_{\text{BG}} - N_{\pi^0 \pi^0}^F}{\epsilon_{\pi^0 \pi^0} N_{\bar{p}} (1 - F)}, \quad (1)$$

where  $N_{\pi^0 \pi^0}$  is the number of  $\pi^0 \pi^0$  reconstructed events,  $\epsilon_{\pi^0 \pi^0}$  the reconstruction efficiency,  $N_{\text{BG}}$  the background events,  $N_{\pi^0 \pi^0}^F$  the  $\pi^0 \pi^0$  events produced in-flight,  $N_{\bar{p}}$  the number of  $\bar{p}$  annihilations inside the target, and  $F$  the fraction of in-flight  $\bar{p}$  annihilations. Each term has been evaluated in at least two independent ways. The strategy of the analysis, as well as the codes used for event selection, filtering, reconstruction and efficiency calculation, is the same as already exploited in the previous  $f(\pi^0 \pi^0, \text{NTP})$  analysis [1].

In Secs. II, III, IV and V, the apparatus and the  $\pi^0 \pi^0$  analysis of the neutral data sample are described. Sections VI and VII contain, respectively, the study of the  $\pi^0 \eta$  annihilation frequency and the analysis of the MB sample. In Sec. VIII, we discuss the present experimental situation by considering the latest published results.

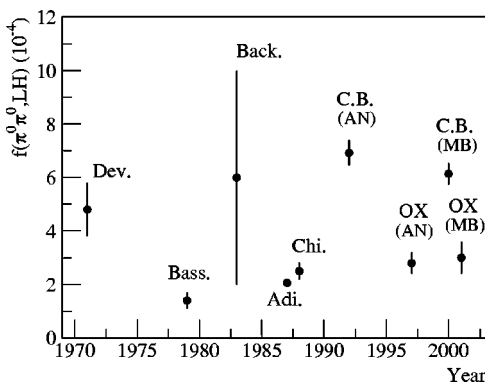


FIG. 1. The present experimental situation of the protonium annihilation frequency in liquid hydrogen [ $f(\pi^0 \pi^0, \text{LH})$ ]. For details on symbols and references see text and Table I.

## II. APPARATUS AND DATA TAKING

The  $\pi^0 \pi^0$  and  $\pi^0 \eta$  measurements were performed by stopping the antiproton beam from the LEAR facility at CERN in a cooled cylindrical liquid hydrogen target (15 cm diameter, 25 cm long). The antiprotons crossed in sequence a plastic scintillator, a collimator and a Si-detector (4 cm diameter, 300  $\mu\text{m}$  thick) placed 40 cm from the target center. The target and the beam line were the same, suitably adapted, used in the  $\bar{n}$  data taking [15,16]. The antiprotons were selected by requiring the coincidence of the signals from the scintillator and the Si-detector. The detector configuration, composed by the time-of-flight system (TOF), the drift chamber (JDC) and the high angular resolution gamma detector (HARGD) [17], was the same as that of the  $\pi^0 \pi^0$  measurement performed by Obelix in NTP conditions [1]. The present work is based on  $N_{\text{AN}} = 6.354 \times 10^6$  annihilation events collected with an all-neutral (AN) trigger, requiring an antiproton entering the target and no signals from the TOF scintillators. A pre-scaled sample of MB events ( $N_{\text{MB}}^P = 0.25 \times 10^6$ ) was also recorded during the AN runs in order to monitor the apparatus stability and the vertex position. Another sample of  $N_{\text{MB}} = 0.847 \times 10^6$  MB events was collected in various steps during the data taking period.

## III. THE ANTIPROTON BEAM AND VERTEX DISTRIBUTION

The momentum of the  $\bar{p}$  beam used for these measurements was 305 MeV/c, with a mean free path in the liquid hydrogen target of about 12 cm and negligible straggling.

The vertex distribution along the beam axis ( $z$  coordinate) obtained from the pre-scaled MB events is shown in Fig. 2. The vertices were almost completely contained in the target, therefore the  $\bar{p}$  in-wall annihilations were negligible. The standard deviation of the distribution (about 1 cm in the  $z$  coordinate) is almost entirely due to the resolution in the  $z$  vertex reconstruction.

The number of annihilations inside the target ( $N_{\bar{p}}$ ) has been determined by three independent methods, by exploiting the information of the MB runs and the beam scalars:

- (i) We have evaluated  $N_{\bar{p}}$  in the MB sample by flagging

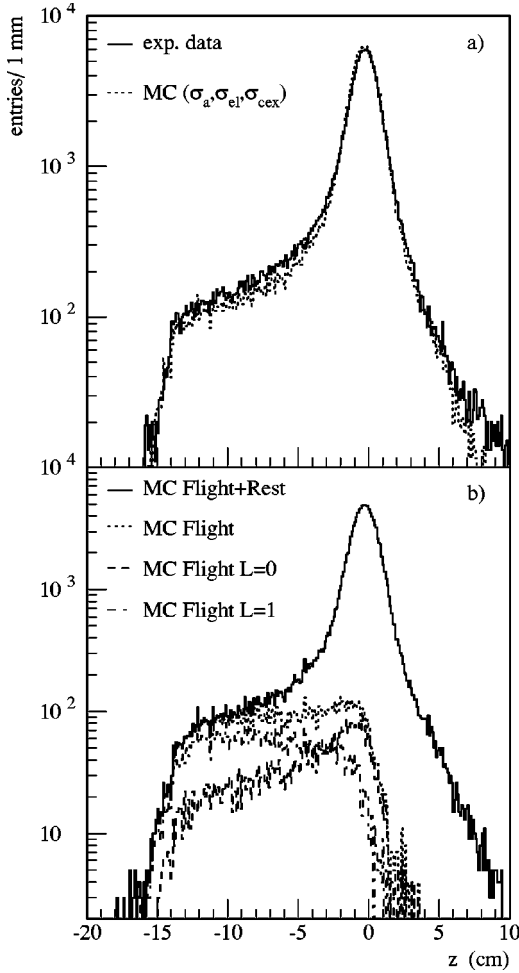


FIG. 2.  $z$  vertex distribution of all the observed annihilations. The agreement between Monte Carlo and experimental data is shown in graph (a). Graph (b) shows the various in-flight contributions. The target is placed approximatively at  $-14 \text{ cm} \leq z \leq 11 \text{ cm}$ .

all the events which satisfy the neutral trigger condition. In this way,  $N_{\bar{p}}$  can be calculated as the ratio between the total number of AN events  $N_{\text{AN}}$  and the neutral trigger frequency defined as  $\epsilon_{\text{AN}} = (N_{\text{AN}})_{\text{MB}} / N_{\text{MB}}$ , where  $(N_{\text{AN}})_{\text{MB}}$  represents the number of flagged events. With  $\epsilon_{\text{AN}} = (4.08 \pm 0.02)\%$  the result  $N_{\bar{p}} = (155.7 \pm 0.8) \times 10^6$  is obtained.

(ii) We have applied the same procedure to the MB data, with the neutral trigger frequency evaluated from the beam counting scalers, obtaining  $\epsilon_{\text{AN}} = (3.978 \pm 0.002)\%$  and  $N_{\bar{p}} = (159.74 \pm 0.08) \times 10^6$ .

(iii) Finally, by counting  $N_{\bar{p}}$  directly from the beam scal-

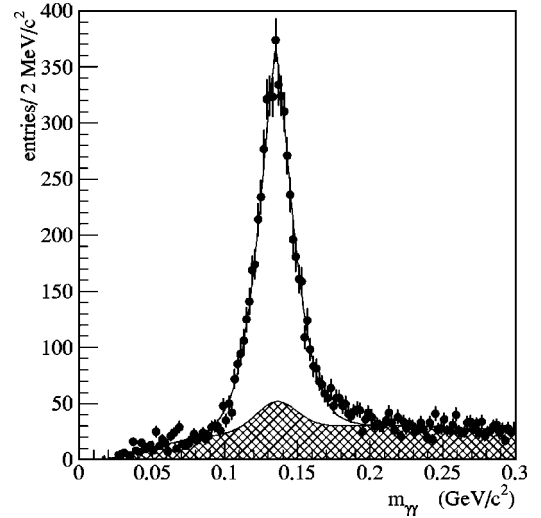


FIG. 3. The  $\gamma\gamma$  invariant mass distribution of the combinations passing the 1C fit cuts. The peak is centered at  $135.2 \pm 0.3 \text{ MeV}/c^2$  and has a full width at half maximum of  $24 \pm 1 \text{ MeV}/c^2$ . The filled graph represents the background fit corrected to account for the combinatorial effect.

ers on the AN data, we have obtained  $N_{\bar{p}} = 160.56 \times 10^6$ .

The values resulting from the three procedures are in reasonable agreement; we took an average value of  $N_{\bar{p}} = (160 \pm 4) \times 10^6$ , where the quoted error is a conservative estimation of the systematic uncertainty.

The contribution of in-flight annihilations ( $F$ ) has been established in two independent ways. First of all, we have calculated the in-flight annihilation probability in an analytic way. The probability of the  $\bar{p}$  to interact with the target has been evaluated using the most recent measurements of the in-flight annihilation cross sections [18] and the stopping power at very low energy [19]. In this way, a contribution at a level of  $(10 \pm 1)\%$  has been obtained. As a second step, we have performed a detailed Monte Carlo simulation based on the GEANT 3.15 package [20], which was developed to simulate the Obelix beam line, the apparatus and the antiproton interactions, taking into account all the active and passive materials. The main antiproton interactions inside the target (such as annihilation, elastic scattering, charge exchange and ionization) have been included by exploiting the recent experimental results cited above. The  $\bar{p}$  vertex distribution obtained from this simulation can be compared with the real data after applying a smearing to take into account the vertex reconstruction resolution. As shown in Fig. 2(a), the two distributions are in excellent agreement; the various in-flight annihilation contributions from the  $L=0$  and  $L=1$  proto-

TABLE II. Results of the fit procedure applied to the AN sample. The adopted cuts are:  $\chi^2 \leq 1.64$ ,  $Q_{\pi^0} \geq 0.3$  and  $Q_{\gamma\gamma} \geq 0.3$  for the 1C fit;  $\chi^2 \leq 3.22$ ,  $Q_{\pi^0} \geq 0.3$  and  $Q_{\pi^0} \geq 0.3$  for the 2C fit.

Fit	$N_{\pi^0\pi^0} - N_{\text{BG}}$	$\epsilon_{\pi^0\pi^0}(\%)$	$N_{\pi^0\pi^0}^F$	$f(\pi^0\pi^0, \text{LH}) (\times 10^{-4})$
1C	$4661 \pm 90$	$11.2 \pm 0.1$	$230 \pm 25$	$2.8 \pm 0.1$
2C(A)	$2634 \pm 94$	$6.18 \pm 0.08$	$140 \pm 15$	$2.8 \pm 0.1$
2C(B)	$2529 \pm 70$	$6.18 \pm 0.08$	$140 \pm 15$	$2.7 \pm 0.1$

nium waves are shown in Fig. 2(b). The in-flight annihilation probability results in  $F = (10.1 \pm 0.1_{\text{stat}} \pm 0.4_{\text{syst}})\%$ , in complete agreement with the analytical method.

#### IV. THE $\pi^0\pi^0$ ANALYSIS

The evaluation of the number of  $\pi^0\pi^0$  events, of the background and of the reconstruction efficiency have been performed by selecting in the AN sample the events with four clusters in HARGD, no tracks in the JDC and no hits in the TOF. The gamma directions have been obtained by connecting the photon conversion points to the vertex evaluated from the pre-scaled MB events. Then, two kinematic fits, with one (1C) and two (2C) constraints, have been applied to the selected events in order to test the hypotheses  $\bar{p}p \rightarrow \pi^0\gamma\gamma \rightarrow 4\gamma$  (6 possible combinations per event) and  $\bar{p}p \rightarrow \pi^0\pi^0 \rightarrow 4\gamma$  (3 possible combinations per event), respectively.

In Fig. 3, the  $\gamma\gamma$  invariant mass distribution from the 1C fit is shown for combinations satisfying the cuts  $\chi^2 \leq 1.64$ ,  $Q_{\pi^0} \geq 0.3$  and  $Q_{\gamma\gamma} \geq 0.3$ , where  $\chi^2$  is the chi-square of the 1C fit,  $Q_{\pi^0}$  is the cumulative distribution of the  $\pi^0$  decay opening angle and  $Q_{\gamma\gamma}$  is the cumulative distribution of the opening angle of the free  $\gamma\gamma$  couple [1]. The spectrum has been fitted to the function

$$F = A \exp\left(-\left|\frac{m_{\gamma\gamma} - \mu}{\sqrt{2}\sigma}\right|^\delta\right) \quad (2)$$

to reproduce the  $\pi^0$  peak [1] plus a polynomial curve (dashed part of the histogram) for the background, corrected in order to take into account the combinatorial effect due to the possibility that a single event enters twice in the histogram. With these cuts 4661  $\pi^0\pi^0$  combinations (background subtracted) have been counted, on a background contribution at the 20% level evaluated directly from the plot. The result obtained is listed in the second column of Table II.

The 2C kinematic fit allows to extract the  $\pi^0\pi^0$  event from the sample by constraining both  $\gamma\gamma$  couples to the  $\pi^0$  mass. Different cuts on  $\chi^2$  and  $Q_{\pi^0}$  have been applied to have a good signal/noise ratio and to check the stability of the results. By requiring  $\chi^2 \leq 3.22$ ,  $Q_{\pi^0_1} \geq 0.3$  and  $Q_{\pi^0_2} \geq 0.3$ , we have selected 3125  $\pi^0\pi^0$  events. In Fig. 4 the  $\gamma\gamma$  invariant mass (a) and momentum (b) distributions of the events passing the above mentioned cuts are shown.

Although the 2C fit is more selective, the background contribution cannot be evaluated directly from the experimental spectra as for the 1C fit; in the present case, it has been determined with two completely independent methods already used in previous analyses [1,21]:

(a) We have generated the main background annihilation reactions (e.g.  $3\pi^0$ ,  $4\pi^0$ ,  $5\pi^0$ ,  $\pi^0\eta$ ,  $\pi^0\omega$ ,  $2\pi^0\eta$  and  $2\pi^0\omega$ ) using the Monte Carlo code of the apparatus (described below). Moreover the  $\bar{p}p \rightarrow 3\pi^0$  reaction has been simulated by taking into account the dynamics of the annihilation as measured by other experiments [7]. Then we have applied the above analysis to these reactions in order to obtain the rejection power for each channel [21]. The results

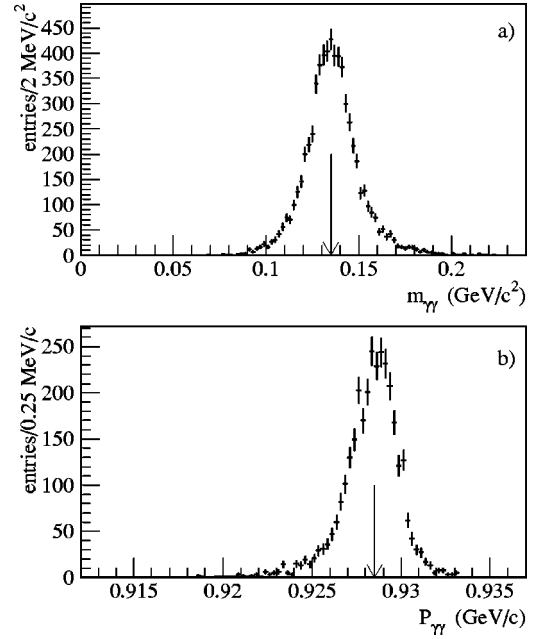


FIG. 4. The  $\gamma\gamma$  invariant mass (a) and momentum distribution (b) of the events passing the 2C fit cuts. The invariant mass and momentum peaks are centered at 135 MeV/c<sup>2</sup> and 928.3 MeV/c, respectively. The momentum peak is characterized by a full width half maximum  $\Delta P_{FWHM} = 3.2$  MeV/c.

obtained are summarized in Table III, where the last column reports the number of background events  $N_{\text{BG}}$  for our sample, evaluated through the following formula:

$$N_{\text{BG}} = \sum_x N_{\text{BG}}^x = N_{\bar{p}} \sum_x f(\bar{p}p \rightarrow x) \epsilon_x, \quad (3)$$

where  $N_{\bar{p}}$  is the antiproton number and  $N_{\text{BG}}^x$ ,  $f(\bar{p}p \rightarrow x)$  and  $\epsilon_x$  are, respectively, the number of background events, the experimental annihilation frequency and the reconstruction efficiency of the  $x$  reaction subjected to the  $\pi^0\pi^0$  hypothesis. This procedure results in a determination of  $491 \pm 75$  background events, corresponding to a background contribution of  $(16 \pm 2)\%$ , which is mainly given by the  $3\pi^0$  reaction.

(b) We have fitted the  $\chi^2$  distribution of the experimental data as a combination of a signal contribution and a background one, the shapes of these components being determined by a study of the corresponding MC distributions. The situation is presented in Fig. 5. With this method we find  $596 \pm 25$  events, corresponding to a background contribution of  $(19 \pm 1)\%$ , in agreement with the previous result.

In order to determine the reconstruction efficiency  $\epsilon_{\pi^0\pi^0}$ , we have generated a sample of about  $10^5$   $\pi^0\pi^0$  Monte Carlo events based on the GEANT 3 package (version 3.21) [20]. Each of the detectors has been included in the simulation, its intrinsic efficiency being evaluated both on samples of  $\bar{p}p$  data and on cosmic muons collected in the same period of the AN data sample. The  $\pi^0\pi^0$  reaction has then been simulated at rest as well as in flight. The events have been submitted to the same analysis chain of the real data. With the cuts mentioned above, we find that the reconstruction effi-



TABLE III. Principal background sources for the  $\pi^0\pi^0$  2C(A) fit. Each row lists, in sequence, the type of reaction, the total annihilation frequency, the annihilation frequency for the final states involving only  $\gamma$ 's, the number of generated events, the probability ( $\epsilon_x$ ) of reconstructing the reaction as  $\pi^0\pi^0$  and the number of background events for the present AN sample.

Reaction	$f (\times 10^{-4})$	$f \text{ sim. } (\times 10^{-4})$	Events sim.	$\epsilon_x (\times 10^{-4})$	Exp. BG events
$3\pi^0$	$60 \pm 10$	$60 \pm 10$	500 k	$5.3 \pm 0.3$	$368 \pm 66$
$4\pi^0$	$100 \pm 50$	$100 \pm 50$	500 k	$0.44 \pm 0.09$	$68 \pm 34$
$5\pi^0$	$71 \pm 10$	$71 \pm 10$	100 k	$0.02 \pm 0.02$	$2 \pm 2$
$\pi^0\eta$	$2.1 \pm 0.1$	$0.8 \pm 0.1$	100 k	$0.30 \pm 0.17$	$< 1$
$2\pi^0\eta$	$75 \pm 8$	$29 \pm 3$	500 k	$0.32 \pm 0.08$	$15 \pm 5$
$\pi^0\omega$	$53.7 \pm 4.7$	$4.6 \pm 0.4$	100 k	$4.3 \pm 0.7$	$32 \pm 5$
$2\pi^0\omega$	$200 \pm 21$	$17 \pm 2$	200 k	$0.2 \pm 0.1$	$5 \pm 3$

ciency for  $\bar{p}p \rightarrow \pi^0\pi^0$  corresponding to the 1C and the 2C fits is, respectively,  $\epsilon_{\pi^0\pi^0}^{1C} = (11.2 \pm 0.1)\%$  and  $\epsilon_{\pi^0\pi^0}^{2C} = (6.18 \pm 0.08)\%$ , where the error quoted is the statistical one (see the third column of Table II).

In order to check the reliability of the Monte Carlo, we have performed detailed studies on the single photon detection efficiency exploiting both real and Monte Carlo data. On a MB sample collected in the same period we have selected the  $\pi^+\pi^-\pi^0$  final state by fitting the events to the hypothesis  $\pi^+\pi^-\pi_{\text{miss}}^0$  (one constraint fit). Strong quality cuts have been applied to make the background contribution negligible. Of the selected events we have considered those including at least one detected  $\gamma$  and have checked whether HARGD detected the other  $\gamma$  or not. The  $\gamma$  detection efficiency has been defined as the ratio between the number of detected  $\gamma$ 's and of the number of expected  $\gamma$ 's at their energy, evaluated by means of simple kinematic considerations. As a result, we find a complete agreement between Monte Carlo and experimental data (see Fig. 6), confirming the reliability of the calorimeter simulation.

Finally, the number of  $\pi^0\pi^0$  events coming from in-flight annihilations [ $N_{\pi^0\pi^0}^F$  of Eq. (1)] has been determined both by an analytic calculation and by a Monte Carlo simulation. In

the latter case we have generated  $\bar{p}$ 's with momentum varying from 305 MeV/c to few MeV/c, forcing them to annihilate in flight in a  $\pi^0\pi^0$  final state, and we have analyzed these events with the 1C fit method. In both ways, we obtain a background contribution of about 5%. The results are summarized in the fourth column of Table II.

## V. $\pi^0\pi^0$ ANNIHILATION FREQUENCY AND SYSTEMATIC ERROR

The results of the analysis on the  $\pi^0\pi^0$  annihilation frequency are reported in the last column of Table II. They are in excellent agreement, yielding the final result

$$f(\pi^0\pi^0, \text{LH}) = (2.8 \pm 0.1_{\text{stat}} \pm 0.4_{\text{sys}}) \times 10^{-4}. \quad (4)$$

We have performed detailed studies to evaluate the systematic errors and to check the stability and the reliability of our result. Concerning the systematic uncertainties, we have considered mainly the following items:

(a) Quality cuts. We have checked the stability of the result against variations of the selection cuts as  $\chi^2$ ,  $Q_{\pi^0}$  and  $Q_{\gamma\gamma}$ ; the maximum fluctuation of the annihilation frequency

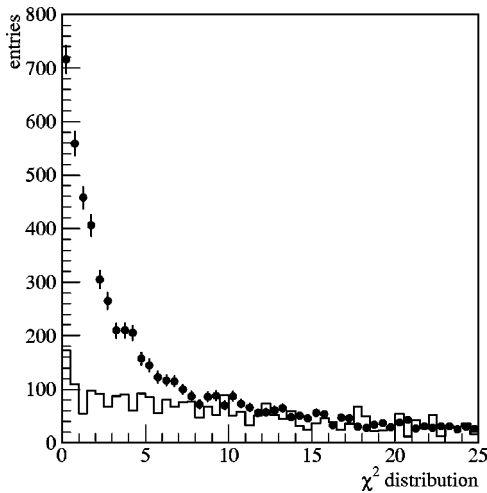


FIG. 5.  $\chi^2$  distribution of the fit 2C for real data (points with error bars) and Monte Carlo background (solid line).

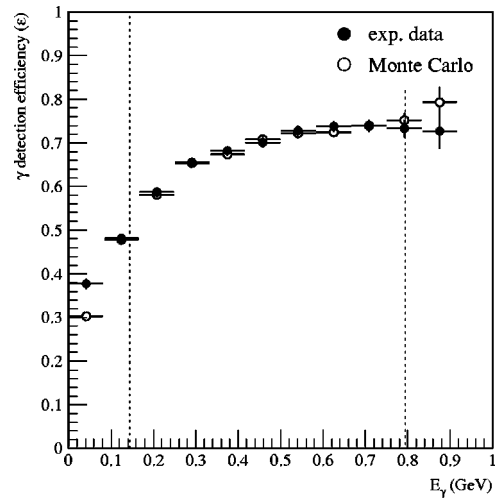


FIG. 6.  $\gamma$  detection efficiency ( $\epsilon$ ). With the cuts used in the  $\pi^0\pi^0$  analysis, the region of interest is delimited by dotted lines.

value has been found at a level of 9%, which has been included in the systematic error.

(b) Monte Carlo simulation parameters. We have performed systematic studies on the detection efficiency by varying the input parameters in the Monte Carlo calculation. Intrinsic Limited Streamer Tube (the active material of HARGD) efficiencies and multi-hit probability have been varied in a wide range. We have found that, although the average number of hits detected per single gamma is sensitive to these changes, the detection efficiency to the  $\pi^0\pi^0$  reaction is stable. The Monte Carlo simulation has also been checked by comparing the expected  $\gamma$  angular distribution from  $\pi^0\pi^0$  to the experimental one. From these studies we have found a relative systematic error of 2.5% in  $\epsilon_{\pi^0\pi^0}^{\text{MC}}$ .

(c) Antiproton number. Annihilations on the Si-detector have also been considered, and found to be negligible at a level of 0.1%. By comparing the different methods for determining the incoming beam, we have computed a relative systematic error of 2.5% in the antiproton number  $N_{\bar{p}}$ .

(d) Electronic noise. Noise reduction techniques have been employed both at the hardware and analysis level. Pick-up noise in the JDC and HARGD detectors was strongly reduced by means of an RF antenna used to inhibit data acquisition in the presence of environment noise. TOF signals (used both in the trigger and in the analysis) were defined by a timed coincidence of two photomultipliers placed at both ends of each scintillator slab. In the analysis, only runs showing stability on beam, trigger and detectors behavior have been considered. Finally, the residual noise contribution has been determined through the analysis of the  $\bar{p}p \rightarrow \pi^+\pi^-, K^+K^-$  reactions, performed on MB data. By studying the fraction of more than two hit slabs in the TOF, an upper limit of the electronic noise to the systematic error has been found at a level of 1.5%.

The total systematic error of 16% has been determined by taking into account all these effects.

A detailed analysis has also been performed on the stability and reliability of the  $f(\pi^0\pi^0, \text{LH})$  result, which can be summarized in the following steps.

(a) Selection type. We have performed a systematic study on the time stability by splitting the AN sample in many sub-samples. As an example, we report here the results obtained after a subdivision into two samples of about 3 million events each:

$$f(\pi^0\pi^0, \text{LH, set 1}) = (2.83 \pm 0.12_{\text{stat}}) \times 10^{-4}, \quad (5)$$

$$f(\pi^0\pi^0, \text{LH, set 2}) = (2.77 \pm 0.13_{\text{stat}}) \times 10^{-4}. \quad (6)$$

Here the label ‘‘set 1’’ (‘‘set 2’’) refers to the events in the first (second) half of the AN data acquisition.

We have also checked the uniformity of the result with respect to the HARGD acceptance, by evaluating the annihilation frequency separately for two supermodule couples [17]. By considering, for example, the couples of top/bottom (T/B) and left/right (L/R) supermodules, we obtain the following determinations of  $f(\pi^0\pi^0)$ :

$$f(\pi^0\pi^0, \text{LH, T/B}) = (2.95 \pm 0.1_{\text{stat}}) \times 10^{-4}, \quad (7)$$

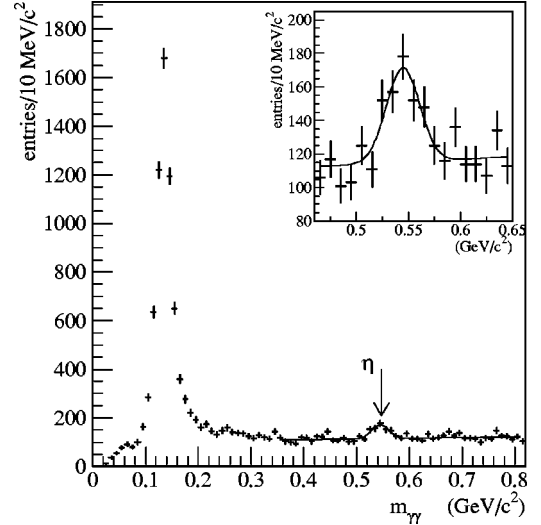


FIG. 7. The  $\gamma\gamma$  invariant mass distribution of the combinations passing the 1C-fit cuts for the whole spectrum and for the  $\eta$  mass region (shown in the inset). The  $\eta$  peak is centered at  $545 \pm 3$  MeV/ $c^2$  and it has a width of  $15.5 \pm 2.5$  MeV/ $c^2$ .

$$f(\pi^0\pi^0, \text{LH, L/R}) = (2.75 \pm 0.1_{\text{stat}}) \times 10^{-4}. \quad (8)$$

(b) Different trigger sample. The value of  $f(\pi^0\pi^0, \text{LH})$  has also been evaluated from the pre-scaled MB data by applying the 2C-fit hypothesis with the same criteria described before. The number of  $\bar{p}$ 's, which coincides with the number of recorded events, is, in this case,  $N_{\text{MB}} = 8.47 \times 10^5$ , while for the in-flight  $\bar{p}$  annihilation fraction  $F$  we have assumed the same value used in the AN sample. The reconstruction efficiency and the background contribution have been re-evaluated in the same way as in the 2C fit of the previous analysis, obtaining the same values. At the end, with the same cuts as before,  $14 \pm 3.7$  events, with a background contribution at the 16% level, are selected, leading to

$$f(\pi^0\pi^0, \text{LH, MB_I, 2C}) = (2.4 \pm 0.8_{\text{stat}}) \times 10^{-4}, \quad (9)$$

where the error is statistical only. The new result, though less precise due to the poorer statistics, is in agreement with the previous determination obtained in completely independent trigger conditions.

## VI. $\pi^0\eta$ ANNIHILATION FREQUENCY

Using the AN sample we have also determined the annihilation frequency of the reaction  $\bar{p}p \rightarrow \pi^0\eta$ , by exploiting the  $\eta \rightarrow \gamma\gamma$  decay mode [ $\text{BR}(\eta \rightarrow \gamma\gamma) = (39.33 \pm 0.25)\%$  [22]]. The whole strategy of the analysis, as well as the determination of the background, of the in-flight annihilations and of the systematic uncertainties, is the same as that applied in the 1C-fit  $\pi^0\pi^0$  analysis. We have selected events requiring four clusters in the HARGD, no tracks in the JDC and no hits in the TOF. Then we have applied the 1C fit to test the hypothesis  $\bar{p}p \rightarrow \pi^0\gamma\gamma \rightarrow 4\gamma$  and have studied the invariant mass of the two gammas in the  $\eta$  mass region. Figure 7 shows the 1C-fit  $\gamma\gamma$  invariant mass distribution for

the whole spectrum and a zoom in the  $\eta$  region mass. The  $\eta$  signal can be clearly seen, with a mass peak centered around the expected value. With this method  $N_{\pi^0\eta}=(182\pm 37)$  events have been counted after the background subtraction whose contribution has been directly obtained from the  $\gamma\gamma$  invariant mass spectrum. The reconstruction efficiency ( $\epsilon_{\pi^0\eta}$ ) has been determined by generating  $10^5$   $\pi^0\eta$  events, forcing the decay  $\eta\rightarrow\gamma\gamma$  and applying the same analysis and cuts used for the experimental data. As a result, the value  $\epsilon_{\pi^0\eta}^{1C}=(3.6\pm 0.2)\%$  has been obtained. Within the same simulation, we have also calculated the  $\pi^0\eta$  in-flight annihilation, with a result at the 2% level. The number of  $\bar{p}$ 's and the in-flight annihilation fraction are obviously the same as in the  $\pi^0\pi^0$  analysis. Finally, the value obtained for the  $\pi^0\eta$  annihilation frequency is

$$f(\pi^0\eta, \text{LH})=(0.9\pm 0.2_{\text{stat}}\pm 0.1_{\text{sys}})\times 10^{-4}. \quad (10)$$

We have checked the stability of this result with respect to variations of the selection cuts, without finding any systematic fluctuations. The systematic error evaluation follows from the same considerations as in the  $\pi^0\pi^0$  analysis.

## VII. ANALYSES ON MB DATA

A completely independent evaluation of the  $\pi^0\pi^0$  annihilation frequency has been performed on a MB sample collected in a liquid hydrogen target with a different apparatus setup. The measurement was performed by stopping 201 MeV/c momentum antiprotons in a smaller cylindrical hydrogen target (1.7 cm diameter, 4.4 cm long), surrounded by the vertex detector (SPC), not present in the previous measurement. The beam setup was composed by a plastic scintillator, a collimator and a Si-detector placed just in front of the target. The rest of the detector was the same as previously described. With this configuration we collected  $3.2\times 10^6$  MB events. Using this sample, we have also decided to make a detailed study on the annihilation frequency of the  $\pi^+\pi^-$  and  $\pi^+\pi^-\pi^0$  channels, for which several values can be found in the literature. This study has allowed an estimation of the possible systematic effects of each single term of Eq. (1) (for details of these analyses, see Ref. [23]).

The evaluation of  $N_{\bar{p}}$  and the fraction of the in-flight annihilations are the same for all the reaction channels. Due to the small dimension of the target, a determination of the annihilations out of the target walls, which were negligible for the  $\pi^0\pi^0$  analysis performed on the AN sample, becomes necessary. The fractions of in-flight and out-of-target annihilations have been evaluated by comparing the vertex distribution along the beam line as obtained by a Monte Carlo simulation with the corresponding experimental distribution. This detailed Monte Carlo simulation has followed the lines described in Sec. III taking into account all the low-energy hadronic interaction cross-sections inside the new beam line and the target. The contribution of the in-flight annihilations is  $F=(2.61\pm 0.06)\%$ , this value being smaller than the one of the  $\pi^0\pi^0$  analysis because of the shorter antiproton path (about 1 cm). The percentage of the out-of-target annihilations has been determined as  $(5.98\pm 0.05)\%$ . Taking into

account this effect the value  $N_{\bar{p}}=(3.003\pm 0.002)\times 10^6$  has been obtained.

The  $\pi^+\pi^-$  annihilation frequency was determined by selecting events with two opposite charged tracks in the JDC and by submitting them to a four-constraint kinematic fit (4C) testing the hypothesis  $\bar{p}p\rightarrow\pi^+\pi^-$ . By applying the quality cut  $P(\chi^2)>0.3$  on the  $\chi^2$  probability of the fit, we selected  $3039\pm 55$  events. The Monte Carlo reconstruction efficiency was determined by applying the same analysis procedure and selection cuts to the simulated events, with the result  $\epsilon_{\pi^+\pi^-}^{4C}=(33.40\pm 0.14)\%$ . The background contribution coming from  $K^+K^-$  and  $\pi^+\pi^-\pi^0$  annihilations was found to be negligible ( $N_{\text{BG}}\approx 5$  events). Finally, the  $\pi^+\pi^-$  annihilation frequency turned out to be

$$f(\pi^+\pi^-, \text{LH, MB\_II})=(31.1\pm 0.6_{\text{stat}})\times 10^{-4}, \quad (11)$$

in good agreement with the previous measurements [24–27].

The annihilation frequency of the reaction  $\bar{p}p\rightarrow\pi^+\pi^-\pi^0$  has been determined by selecting the events in two different ways: first of all, under the hypothesis  $\pi^+\pi^-\pi_{\text{miss}}^0$  (1C fit), just by considering the charged particles in the final state while neglecting all the information on the  $\pi^0$  in the final state. Successively, we have checked the hypothesis  $\pi^+\pi^-\gamma\gamma$  (2C fit) by using also HARGD to detect the  $\gamma$ 's. For the 1C fit hypothesis, we have selected events with two opposite charged tracks having a reconstructed vertex, and have applied to these events the quality cut  $P(\chi^2)>0.2$  on the  $\chi^2$  probability of the fit. We obtained:

$$f(\pi^+\pi^-\pi^0, \text{LH, MB\_II, 1C})=(57.3\pm 0.4_{\text{stat}})\times 10^{-3}. \quad (12)$$

In the 2C-fit analysis we have adopted the same criterion as in the 1C fit for the selection of the charged particles, with the additional requirement of two neutral clusters detected on HARGD. The result is

$$f(\pi^+\pi^-\pi^0, \text{LH, MB\_II, 2C})=(57.0\pm 1.0_{\text{stat}})\times 10^{-3}. \quad (13)$$

The two values are in agreement with each other and with the existing experimental results [see for example the average value  $(54.9\pm 2.3)\times 10^{-3}$  quoted in Ref. [6]].

After all these checks, we have performed on the same sample the measurement of the  $\pi^0\pi^0$  annihilation frequency. The events, selected as previously described, have been submitted both to a 1C fit for the hypothesis  $\bar{p}p\rightarrow\pi^0\gamma\gamma\rightarrow 4\gamma$  and to a 2C fit for the hypothesis  $\bar{p}p\rightarrow\pi^0\pi^0\rightarrow 4\gamma$ . For both analyses, the value of  $N_{\bar{p}}$  and the fraction of the in-flight and out-of-target annihilations are the same as before.

For the 1C-fit analysis we have applied the quality cuts  $\chi^2<1.64$ ,  $Q_{\gamma\gamma}\geq 0.3$  and  $Q_{\pi^0}\geq 0.3$ .

In Fig. 8 the 1C-fit  $\gamma\gamma$  invariant mass distribution is shown for events satisfying the previous cuts. The spectrum has been fitted to a Gaussian-plus-polynomial curve (dashed part of the histogram) corrected in order to take into account the combinatorial effect. The number of events selected after the background subtraction is  $76\pm 14$ . The Monte Carlo re-

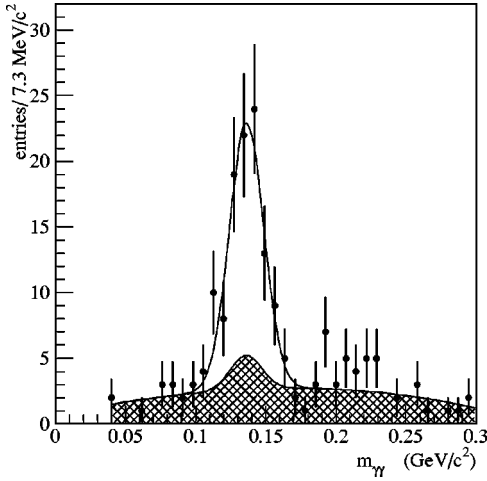


FIG. 8. The  $\gamma\gamma$  invariant mass distribution of the combinations passing the 1C fit cuts applied to the minimum bias sample (MB\_II).

construction efficiency is  $\epsilon_{\pi^0\pi^0}^{1C} = (9.0 \pm 0.1)\%$  and the background contribution  $\sim 28\%$ . The result of the 1C fit analysis is:

$$f(\pi^0\pi^0, \text{LH, MB\_II, 1C}) = (2.9 \pm 0.6_{\text{stat}}) \times 10^{-4}. \quad (14)$$

For the 2C fit analysis, we have selected  $54 \pm 7$  events by applying the quality cuts  $\chi^2 < 3.22$ ,  $Q_{\pi_1^0} \geq 0.3$  and  $Q_{\pi_2^0} \geq 0.3$ . The background has been determined, using the same technique described in Sec. IV (method a), as consisting of  $12.4 \pm 1.8$  events. The Monte Carlo reconstruction efficiency is  $\epsilon_{\pi^0\pi^0}^{2C} (4.62 \pm 0.07)\%$ . The resulting annihilation frequency is

$$f(\pi^0\pi^0, \text{LH, MB\_II, 2C}) = (3.1 \pm 0.6_{\text{stat}}) \times 10^{-4}, \quad (15)$$

which is compatible with the value obtained from the 1C fit.

## VIII. CONCLUSIONS

### A. The $f(\pi^0\pi^0, \rho)$ situation

In this paper, we have presented five different determinations of the  $\pi^0\pi^0$  annihilation frequency in LH (see Table IV) obtained by the Obelix experiment. As denoted by their consistency, the results are independent of differences in trigger condition, period of acquisition and apparatus setup.

TABLE IV. Results for the  $\pi^0\pi^0$  annihilation frequency, obtained by Obelix from different analyses and data samples, as described in this paper.

Trigger	Fit	$f(\bar{p}p \rightarrow \pi^0\pi^0, \text{LH}) \times (10^{-4})$
All-Neutral	1C	$2.8 \pm 0.1_{\text{stat}}$
All-Neutral	2C	$2.8 \pm 0.1_{\text{stat}}$
MB_I	1C	$2.4 \pm 0.8_{\text{stat}}$
MB_II	1C	$2.9 \pm 0.6_{\text{stat}}$
MB_II	2C	$3.1 \pm 0.6_{\text{stat}}$

They are, moreover, in good agreement with the results of most of the earlier experiments. On the other hand, they also confirm a disagreement of a factor greater than 2 with previously published results of the Crystal Barrel experiment, which, in turn, are supported by a recent reanalysis of the early LH data samples [9].

Possible experimental origins of this disagreement, which might be attributed to the Obelix experiment, have been considered carefully in the present analysis. Our inspection has included the possibility of an overestimation of the photon detection efficiency, of a problem in the beam counting or a misvaluation of the background sources.

Concerning the detection efficiency, we note that Obelix and Crystal Barrel are the only two experiments in the position of detecting all four photons and of reconstructing exclusively the  $\pi^0\pi^0$  final state. The  $\pi^0\pi^0$  detection efficiency for the Obelix experiment is much smaller than for the Crystal Barrel one, due to the geometry of the apparatus and to the cuts applied in the data analysis. However, Obelix has measured this detection efficiency directly on a MB sample collected in the same experimental conditions of the data used for the study of the annihilation frequency. The results, reported in Sec. VII, show a very good agreement between the data and the Monte Carlo predictions. Furthermore, using the same data sample, the  $\bar{p}\bar{p} \rightarrow \pi^+\pi^-\pi^0$  annihilation frequency has been measured both with and without the requirement of the  $\pi^0$  detection. The good agreement between the two results shows the reliability of the Monte Carlo estimation of the photon detection efficiency. Moreover, the  $f(\pi^+\pi^-, \text{LH})$  result confirms the understanding of charged particle and detector simulation as well as the correctness of the beam evaluation.

Finally, we observe that Obelix has also measured the  $\pi^0\pi^0$  annihilation frequency with a gaseous hydrogen target in NTP conditions (see Table I); a misvaluation of the  $\pi^0\pi^0$  reconstruction efficiency by a factor greater than 2 would be reflected also in this measurement, giving a result  $f(\pi^0\pi^0, \text{GH}) \geq 2 \times 12.7 \times 10^{-4} = 25.4 \times 10^{-4}$ . This value is incompatible with the measurement of the  $\pi^+\pi^-$  annihilation frequency performed by the Asterix experiment in coincidence with protonium x-ray emission. In fact, due to charge symmetry, the following relation applies to the  $\pi^+\pi^-$  and  $\pi^0\pi^0$  annihilation frequencies [3,6]:

$$f(\pi^0\pi^0, \rho) = \frac{1}{2} \alpha_P(\rho) f_X(\pi^+\pi^-), \quad (16)$$

where  $\alpha_P(\rho)$  is the percentage of protonium  $P$ -wave and  $f_X(\pi^+\pi^-)$  is the  $\pi^+\pi^-$  annihilation frequency measured in coincidence with the x ray emission. Taking into account that  $f_X(\pi^+\pi^-) = (48.1 \pm 4.9) \times 10^{-4}$  [28], we get  $\alpha_P(\text{NTP}) \approx 106\%$ , which is a factor of 2 above the current evaluations [3,6] and outside any physical range.

Concerning the counting of the incoming beam, we remark that the beam line configuration and the target used in the AN sample avoided any contamination due to in wall annihilations and any problem due to the lateral shift of the LEAR antiproton beam. Moreover we outline that the two results presented in this paper, obtained respectively from the



AN and from the MB samples, with two different beam line configurations, are in good agreement with each other. In particular, since the dimensions of the target and of the silicon detector, the beam energy as well as the beam evaluation technique were different, possible problems in the measurement of the antiproton beam would have most likely been reflected in the results.

Finally, our result shows a very good stability under many respects. Different kinematic fits and, consequently, different background evaluations have been applied. Careful tests have been performed by splitting the data sample in different sets, by considering only one part of the calorimeter (top/bottom or left/right supermodules) and by changing the cuts applied in the analysis. These studies add a further confirmation of the high level of self-consistency of our measurement.

As a final remark, we point out that there is disagreement also between our measurement of the  $\pi^0\eta$  annihilation frequency and the value, about a factor of 2 larger, published by Crystal Barrel. On the contrary, our evaluation of the ratio  $f(\pi^0\eta, \text{LH})/f(\pi^0\pi^0, \text{LH}) = 0.32 \pm 0.07$  is in good agreement both with the corresponding Crystal Barrel result [8,9] in LH and with the value obtained by the Obelix experiment in gaseous hydrogen NTP conditions [4,29], as is expected according to the predictions of some models [30].

### B. Status of the two-body annihilation frequencies

The present experimental situation is summarized in Table I. The  $\pi^0\pi^0$  annihilation frequency has been measured by seven experiments with liquid hydrogen targets and by two experiments with gaseous targets at different densities. As already mentioned, the situation is contradictory. The liquid hydrogen result by Crystal Barrel is in disagreement by more than a factor of 2 with most of the existing measurements, including the result by Obelix presented in this paper. Adiels *et al.* [13] and Chiba *et al.* [14] obtained quite precise results with inclusive measurements of the photon spectra using dedicated detectors, while the measurements by Crystal Barrel and Obelix were performed by detecting all the four photons. The only two measurements in gaseous hydrogen, performed by Crystal Barrel and Obelix, also gave conflicting results.

A similar situation also occurs in the studies of in-flight antiproton annihilations. The  $\pi^0\pi^0$  final state has been studied in flight with the main goal of searching exotic states. In this context, two different detectors have measured the  $\pi^0\pi^0$  differential cross section in a wide antiproton momentum range. Two results are available at present: one by Dulude *et al.* [33], the other obtained recently with the Crystal Barrel detector [34]. Both the experiments were designed to measure neutral final states and detected all the four photons with a rather high acceptance. The results are compared in Fig. 9, where a clear disagreement appears: the result by Dulude *et al.* is about a factor of 2 smaller than the one by Crystal Barrel over the whole antiproton momentum range.

In order to check the compatibility of the results reported in this paper with the overall experimental situation, we have performed a new analysis of the two-body annihilation fre-

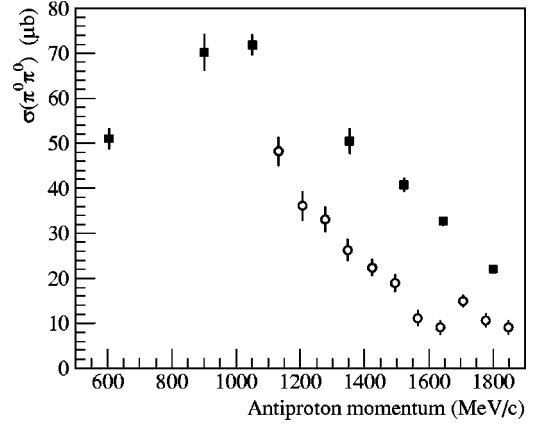


FIG. 9. The cross section  $\sigma(\pi^0\pi^0)$  from in-flight  $\bar{p}p$  annihilations, integrated over the range  $\cos\theta = 0$  to 0.85. Black squares are from the measurement performed with the Crystal Barrel detector [34], open circles are from Dulude *et al.* [33].

quencies in terms of  $P$ -wave annihilation fraction, following the strategy described in Ref. [6]. Referring to the quoted article for the details of the method, we list here the main points of the analysis.

We have considered a number of the annihilation frequencies used in Ref. [6], as well as the results reported in the recent Crystal Barrel publication [9].

In particular, our analysis has included the final states  $\pi^0\pi^0$ ,  $\pi^+\pi^-$ ,  $K^+K^-$ ,  $K_S K_L$ ,  $K_S K_S$ ,  $\eta(1440)\pi^+\pi^-$  and  $\pi^0\eta$ , measured in hydrogen targets at different densities (liquid,  $12\rho_{\text{NTP}}$ , NTP,  $0.005\rho_{\text{NTP}}$  and  $0.002\rho_{\text{NTP}}$ ).

We have considered 27 annihilation frequencies in all and 28 experimental results. For the  $\pi^0\pi^0$  in LH, we have considered the present result and the Crystal Barrel one [9] alternatively.

We have used two different methods to fit the data: one referred to as the “classical” approach [31,32], where the elementary branching ratios of the decays proceeding from the six different protonium hyper-fine levels from which annihilations occur are weighted statistically, the other, based on the model by Batty [3], where the deviation of the population of these levels from the statistical distribution is taken into account through coefficients called *enhancement factors*. In the first case, we have used 13 free parameters in the fit (8

TABLE V.  $\chi^2$ 's per degree of freedom obtained from fits of the existing measurements of the annihilation frequencies. The annihilation frequency  $f(K_S K_L, 12\rho_{\text{NTP}})$  has not been included in the fits. The first fit (Obelix) does not include the  $\pi^0\pi^0$  annihilation frequencies measured by Crystal Barrel in LH and  $12\rho_{\text{NTP}}$  conditions. The second fit (Crystal Barrel) does not include the  $\pi^0\pi^0$  annihilation frequencies measured by Obelix in LH and NTP conditions.

fit method	$\chi^2/\text{d.o.f.}$	
	“classical”	Batty’s model
$\pi^0\pi^0$ from Obelix	20.5/12	10.3/10
$\pi^0\pi^0$ from Crystal Barrel	30.1/12	11.8/10
without $\pi^0\pi^0$ results	20.1/10	8.6/8

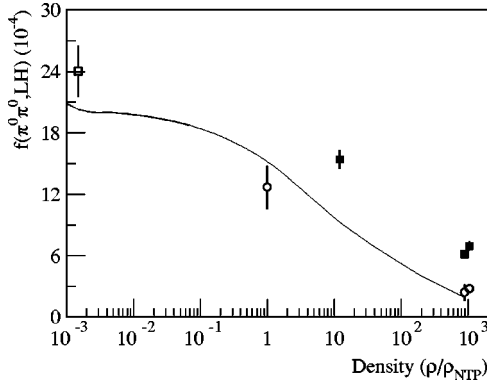


FIG. 10. The  $\pi^0\pi^0$  annihilation frequency as a function of the target density  $\rho$ . Black squares are from Crystal Barrel, open circles from Obelix and open squares from Asterix. The curve has been calculated from a fit of the existing annihilation frequencies using the model by Batty [3].

values of the elementary branching ratios and 5 values of the fraction of the protonium  $P$ -wave annihilations); in the second case, we have fitted the data with 15 free parameters (10 values of the elementary branching ratios and 5 values of the fraction of the protonium  $P$ -wave annihilation).

Least-square fits to these data have been performed in three different configurations: (i) with the  $\pi^0\pi^0$  measurements taken from Obelix only, (ii) with the  $\pi^0\pi^0$  measurements taken from Crystal Barrel only, (iii) without any measurement of the  $\pi^0\pi^0$  annihilation frequency.

The main results of the analysis can be summarized as follows:

The frequency  $f(K_S K_L, 12\rho_{\text{NTP}})$  measured by Crystal Barrel [9] using the MB sample is poorly fitted, with a shift of about three standard deviations. Therefore, we have decided to repeat the fits omitting this value.

The value of  $f(\pi^0\pi^0, \text{NTP})$  measured by Obelix [1] stands below the fit predictions by about  $1.5\sigma$ .

The obtained  $\chi^2$ 's per degree of freedom are given in Table V.

With both approaches, the result by Obelix gives smaller  $\chi^2$ 's than Crystal Barrel.

From the results of the fit performed in configuration (iii) (all the  $\pi^0\pi^0$  results omitted) we can calculate the foreseen values for  $f(\pi^0\pi^0, \rho)$  at different densities. In Fig. 10 the results of the fit performed with the ‘‘enhancement factor’’ approach (model by Batty) are represented by the solid line, while the points refer to the experimental measurements. Almost identical results have been obtained with the ‘‘classical’’ approach. As one can see, the fit of the existing two-body annihilation frequencies favors  $\pi^0\pi^0$  values in agreement with the Obelix measurements, even if the uncertainties in the results are quite large.

For both approaches, it is possible to obtain the  $P$ -wave annihilation fraction  $\alpha_P(\rho)$  at each density as in Ref. [6]. Results from fits in configuration (i) are shown in Table VI. Similar values for  $\alpha_P(\rho)$  are obtained from fit (iii). In the

TABLE VI.  $P$ -wave protonium annihilation fractions for different target densities as obtained from the fits in configuration (i) for both approaches.

target density $\rho$	$\alpha_P(\rho)$	
	‘‘classical’’	Batty’s model
Liquid	$0.12 \pm 0.02$	$0.054 \pm 0.013$
$12 \rho_{\text{NTP}}$	$0.34 \pm 0.07$	$0.34 \pm 0.07$
$\rho_{\text{NTP}}$	$0.60 \pm 0.03$	$0.55 \pm 0.04$
$0.005 \rho_{\text{NTP}}$	$0.86 \pm 0.02$	$0.86 \pm 0.02$
$0.002 \rho_{\text{NTP}}$	$0.86 \pm 0.10$	$0.85 \pm 0.10$

case of configuration (ii), higher values of  $\alpha_P(\rho)$  are obtained especially in LH:  $\alpha_P(\text{LH}) = 0.30 \pm 0.02$  from the ‘‘classical’’ fit and  $\alpha_P(\text{LH}) = 0.12 \pm 0.01$  from the fit performed with Batty’s approach, in close agreement with what has been obtained by Crystal Barrel [9].

### C. Summary

Values of the annihilation frequencies for the reactions  $p\bar{p} \rightarrow \pi^0\pi^0, \pi^0\eta, \pi^+\pi^-$  and  $\pi^+\pi^-\pi^0$  have been measured in liquid hydrogen.

Dedicated checks have been performed on several data sets and with different analysis techniques, in order to evaluate all possible systematic effects as well as the stability of the results.

The photon detection efficiency has been obtained from real data measurements and is well reproduced by Monte Carlo simulations. The  $\pi^0\pi^0$  annihilation frequency has also been obtained from a MB sample in good agreement with the result obtained from the AN sample.

Our measurements are in agreement with those previously obtained by Adiels *et al.* [13] and Chiba *et al.* [14] (see Table I), but are incompatible with the result by Crystal Barrel for a factor of about 2.5. The checks performed on our analysis have not enabled us to find any effect which could account for such a discrepancy.

Our result is also supported by the comparison with previous measurements of the same reaction performed by Obelix in NTP conditions: any change of a factor of 2 in the present result would reflect also in the NTP result giving rise to inconsistencies with the existing  $f(\pi^+\pi^-, \rho)$  measurements [28] and with protonium atomic models.

Finally, we have performed a combined analysis by fitting a set of two-body annihilation frequencies using a least-square method, as described in Refs. [3,4,6,9]. The results obtained show the compatibility of the Obelix measurement with the overall experimental situation.

### ACKNOWLEDGMENTS

We would like to thank C. Batty, B. Pick, U. Wiedner and other members of the Crystal Barrel Collaboration for very useful discussions concerning their annihilation fraction measurements.

- [1] Obelix Collaboration, M. Agnello *et al.*, Phys. Lett. B **337**, 226 (1994).
- [2] C.J. Batty, Rep. Prog. Phys. **52**, 1165 (1989).
- [3] C.J. Batty, Nucl. Phys. **A601**, 425 (1996).
- [4] A. Zoccoli, Phys. At. Nucl. **59**, 1389 (1996).
- [5] C.J. Batty, Nucl. Phys. **A655**, 305c (1999).
- [6] Obelix Collaboration, G. Bendiscioli *et al.*, Nucl. Phys. **A686**, 317 (2001).
- [7] Crystal Barrel Collaboration, V.V. Anisovich *et al.*, Phys. Lett. B **323**, 233 (1994).
- [8] Crystal Barrel Collaboration, C. Amsler *et al.*, Phys. Lett. B **319**, 373 (1993).
- [9] Crystal Barrel Collaboration, A. Abele *et al.*, Nucl. Phys. **A679**, 563 (2001).
- [10] S. Devons *et al.*, Phys. Rev. Lett. **27**, 1614 (1971).
- [11] G. Bassompierre *et al.*, in *Proceedings of the 4th European Antiproton Symposium*, Barr, 1978, edited by A. Fridman (Editions du CNRS, Paris, 1979), Vol. I, p. 139.
- [12] G. Backenstoss *et al.*, Nucl. Phys. **B228**, 424 (1983).
- [13] L. Adiels *et al.*, Z. Phys. C **35**, 15 (1987).
- [14] M. Chiba *et al.*, Phys. Lett. B **202**, 447 (1988).
- [15] M. Agnello *et al.*, Nucl. Instrum. Methods Phys. Res. A **399**, 11 (1997).
- [16] Obelix Collaboration, A. Adamo *et al.*, Phys. Lett. B **287**, 368 (1992).
- [17] S. Affatato *et al.*, Nucl. Instrum. Methods Phys. Res. A **325**, 417 (1993).
- [18] Obelix Collaboration, A. Bertin *et al.*, Phys. Lett. B **369**, 77 (1996).
- [19] Obelix Collaboration, A. Adamo *et al.*, Phys. Rev. A **47**, 4517 (1993).
- [20] R. Brun *et al.*, GEANT3, Internal Report CERN DD/EE/84-1, CERN, 1987.
- [21] Obelix Collaboration, A. Bertin *et al.*, Phys. Lett. B **386**, 486 (1996).
- [22] Particle Data Group, D. Groom *et al.*, Eur. Phys. J. C **15**, 1 (2000).
- [23] Obelix Collaboration, Proceedings of the LEAP2000 Conference, Venice, Italy, 2000 [Nucl. Phys. A (to be published)].
- [24] Crystal Barrel Collaboration, C. Amsler *et al.*, Z. Phys. C **58**, 175 (1993).
- [25] G. Smith, *Proceedings of the Workshop on the Elementary Structure of the Matter*, Les Houches, 1987, edited by J.M. Richard *et al.* (Springer, Berlin, 1988), p. 197.
- [26] C. Baltay *et al.*, Phys. Rev. **145**, 1103 (1966).
- [27] M. Cresti *et al.*, *Proceedings of the International Conference on Elementary Particles*, Siena, 1963 (Soc. It. Fis., Bologna, 1963), Vol. 1, p. 263.
- [28] Asterix Collaboration, M. Doser *et al.*, Nucl. Phys. **A486**, 493 (1988).
- [29] Obelix Collaboration, in *Proceedings of the LEAP94 Conference*, Bled, Slovenia, 1994, edited by G. Kernel *et al.* (World Scientific, Singapore, 1995), p. 97.
- [30] E. Klempt, Phys. Lett. B **308**, 179 (1993).
- [31] G. Reifenröter and E. Klempt, Phys. Lett. B **245**, 129 (1990).
- [32] G. Reifenröter and E. Klempt, Nucl. Phys. **A503**, 885 (1989).
- [33] R.S. Dulude *et al.*, Phys. Lett. **79B**, 329 (1978).
- [34] A.V. Anisovich *et al.*, Phys. Lett. B **468**, 304 (1999); Nucl. Phys. **A662**, 344 (2000).